X-ray tomography based numerical analysis of stress concentrations in non-crimp fabric reinforced composites - assessment of segmentation

Downloaded from: https://research.chalmers.se, 2024-04-25 08:42 UTC

Citation for the original published paper (version of record):

Auenhammer, R., Mikkelsen, L., Asp, L. et al (2020). X-ray tomography based numerical analysis of stress concentrations in non-crimp fabric
reinforced composites - assessment of segmentation methods. IOP Conference Series: Materials Science and Engineering, 942(1). http://dx.doi.org/10.1088/1757-899X/942/1/012038

N.B. When citing this work, cite the original published paper.

research.chalmers.se offers the possibility of retrieving research publications produced at Chalmers University of Technology.
It covers all kind of research output: articles, dissertations, conference papers, reports etc. since 2004.
research.chalmers.se is administrated and maintained by Chalmers Library

(article starts on next page)

IOP Conference Series: Materials Science and Engineering

PAPER • OPEN ACCESS

X-ray tomography based numerical analysis of stress concentrations in non-crimp fabric reinforced composites - assessment of segmentation methods

To cite this article: R M Auenhammer *et al* 2020 *IOP Conf. Ser.: Mater. Sci. Eng.* **942** 012038

View the article online for updates and enhancements.

Recent citations

- Dataset of non-crimp fabric reinforced composites for an X-ray computer tomography aided engineering process
Robert M. Auenhammer *et al*

This content was downloaded from IP address 129.16.69.49 on 26/01/2021 at 15:17

IOP Conf. Series: Materials Science and Engineering **942** (2020) 012038 doi:10.1088/1757-899X/942/1/012038

X-ray tomography based numerical analysis of stress concentrations in non-crimp fabric reinforced composites - assessment of segmentation methods

R M Auenhammer[1,2,*], L P Mikkelsen[2], L E Asp[1] and B J Blinzler[1]

[1]Department of Industrial and Materials Science, Chalmers University of Technology, Hörsalsvägen 7A, SE-41296 Göteborg, Sweden
[2]Department of Wind Energy, Technical University of Denmark, Roskilde, Denmark

E-mail: *robaue@chalmers.se

Abstract. In this study two automated segmentation methodologies of an X-ray computer tomography based numerical analysis are compared. These are then assessed based on their influence on the stress distribution results of finite element models of glass fibre reinforced composites made out of non-crimp fabrics. Non-crimp fabrics reinforced composites are commonly used for wind turbine blades due to their high stiffness to weight ratio for the dominating bending load. Finite element modelling based on X-ray computer tomography allows the reduction of the cost and can accelerate the development process of the key material parameters of wind turbine blades. Recent research progress in the last years has laid the basis for such a procedure. Those processes must be easy applicable, fast and accurate. The main challenge in current methodologies is the segmentation part. The segmentation methods applied for this study have overcome this issue by being automated. This allows for a comparatively fast transfer from X-ray computer tomographic data to finite element results.

1. Introduction

High performance polymer matrix composites are the standard materials used for wind turbine blades due to their durability and the high stiffness to weight ratio. A good fatigue behaviour is especially essential due to the huge amount of load cycles (between 50 and 300 million) [1]. In addition, with increasing blade length, higher tensile stiffness and compression strength are also necessary [2]. The improvement of the composite structure is expensive since it is mostly based on experiments. Finite element modelling based on X-ray computer tomographic data allows to account for real material behaviour


Content from this work may be used under the terms of the Creative Commons Attribution 3.0 licence. Any further distribution of this work must maintain attribution to the author(s) and the title of the work, journal citation and DOI.
Published under licence by IOP Publishing Ltd

after manufacturing of the composite structure. Misaligned and displaced fibres, fibres bundles as well as void formations can be implemented in the model [3].

1.1. X-ray computer tomography

Developed originally for the medical diagnostics field, X-ray computer tomography has expanded its application field to non-medical research and industry in the last decades [4]. This technology allows to create images of the inside of the scanned sample while being non-destructive [5]. The resolutions of modern tomographs can visualise single fibres [6]. X-ray computer tomography scans of composites can be used to assess manufacturing processes, tensile failure, compressive failure and kinking, fatigue as well as impact damage [7].

1.2. X-ray computer tomography image based modelling

X-ray computer tomography image based modelling can improve the quality of finite element analysis [8]. Recent improvements in the images acquisition and analysis allow enhanced applications for evaluating material models and structural improvements of fibre reinforced composites [9]. Increased usage of finite element modelling will reduce the development and production cost for industrial applications. Automated segmentation is in particular important since huge amount of data (in the range up to dozens of Gigabytes), that is generated during X-ray computer tomography, needs to be processed to serve as basis for finite element modelling. The volume of data creates the necessity for automated algorithms which allow accurate, repeatable and cost and time efficient processing. An implementation of the fibre orientation is fundamental for modelling of fibre reinforced composites. X-ray computer tomography can additionally supply the fibre orientation as well. Karamov et al. [10] compared two high-fidelity methods, fibre tracking with the commercial software package Avizo™ and ellipsometry, with a structural tensor approach. Depending on the scanning resolution, high accuracy of the calculated fibre orientation was achieved for all methods in their investigation. The study of Jespersen et al. [11] on the other hand did not include fibre tracking. They focused more on the generation of surface geometries of the single fibre bundles with the application of the commercial software packages Avizo™ and Geomagic Wrap®. The interpolation between single 2D cross-sections resulted in a 3D volume. After the mesh creation, the orientations of the lay-up were used to calculate the material parameters with the Classical-Laminate-Theory. Blinzler et al. [12] conducted a similar study. In contrast to Avizo™ and Geomagic Wrap® they used Solidworks™ to create a 3D surface geometry. With the help of a generated centroid spline for the 3D fibre bundles, the waviness could be accounted for, which is advantageous compared to the study of Jespersen et al. [11]. Both studies however, are manual, time intensive, and depend on the experience of the operator.

1.3. Objective

The goal of this investigation is to assess the influence of the automated segmentation procedures for non-crimp fabrics reinforced composites on the fibre bundle scale on the finite element analysis results. Two methods, called *Physical Boundary* and *Thresholding*

in the following, differing in the representation of the boundary between fibre bundles will be compared in their ability to model stress concentrations.

2. Approach

Glass fibre reinforced composites are used for the highly automated X-ray computer tomography aided process. The fundamental parts for such a process are image acquisition, segmentation and the finite element modelling.

2.1. Material system

Non-crimp fabric glass fibre reinforced composites were manufactured with the architecture Jespersen et al. described in [13]. Four uni-directional bundle layers are placed on each other and each layer is supported by a layer of backing bundles. The composite was manufactured with the vacuum assisted resin transfer moulding technique. An unsaturated polyester was used as the resin. The composite layup with $[b/0, b/0]_s$ was used where the term "b/0" denotes a uni-directional bundles layer oriented at 0° on top of a layer of backing bundles oriented at ±80° (Figure 1).

For the material properties in the finite element analysis, a linear transverse orthotropic

Figure 1: Rendered reconstructed X-ray computer tomographic data of the specimen with a size of $376 \times 936 \times 1708$ pixels and a voxel size of $10.94\,\mu$m displayed in the commercial software package Avizo™ reflecting a physical size of $4.11 \times 10.2 \times 18.7\ mm^3$.

model is chosen. A precis value of the fibre volume fraction is essential for predicting the material parameters. A 2D scanning electron microscopy image of the centre plane of the cross-section was taken of the specimen after it was scanned in the X-ray computer tomograph. The fibre volume fraction was determined based on a image analysis using a threshold operation and taking the ratio of the high intensity glass-fibre pixels to the total amount of pixels in fibre bundle part of the cross-section. The material parameters were calculated based on the fibre volume fraction of 61 % inside the fibre bundles with the

rule of mixtures for the stiffness along fibre direction and Halpin-Tsai for the transverse and shear properties [14]. In Table 1 the values normalised with the longitudinal stiffness can be seen.

Table 1: Calculated material parameters with the Rule of Mixture and Halpin-Tsai normalised with the value of the longitudinal stiffness E_{11}.

E_{11} [-]	E_{22} [-]	E_{33} [-]	G_{12} [-]	G_{13} [-]	G_{23} [-]	ν_{12} [-]	ν_{13} [-]	ν_{23} [-]
1.00	0.265	0.265	0.0775	0.0775	0.0575	0.258	0.258	0.254

2.2. Image acquisition

The central part of the gauge section of a tensile test specimen was scanned at DTU Wind Energy with a 3D X-ray computer tomograph Zeiss Xradia Versa 520 scanner, that has a 2000×2000 pixel detector. A so-called binning of 2 was used. With this setting 2×2 pixels are merged to one pixel. This results in a shorter scanning time but also signifies a lower resolution. Three single scans were stitched together to cover a larger field of view. Further, with the exposure time 4 s, the number of projections 3601, the accelerating voltage 50 kV, the optical magnification $0.4\times$, the voxel size 10.94 μm resulted in a scanning time of approximately 22 h. The voxel size with 10.94 μm is too coarse to resolve single fibres with diameters of 9 and 17 μm. The scanned field of view covers the entire width and thickness of the tensile test specimen. In the main fibre direction, the sample needed to be cropped to reduce the scanning and modelling time. The result is visualised in Figure 1.

2.3. Segmentation method

To investigate the influence of the segmentation method two automated approaches were used. They differ in their complexity and how the boundaries between uni-directional and backing bundles are modelled. Yet, both are comparatively simple considering the goal they need to fulfil. To assure that the segmentation outcomes can be used for accurate finite element modelling, a fibre orientation must be either provided or the assignment possibility must be given. Fundamental to achieving this objective in our approach is a fibre tracking, which was carried out in Avizo™. Based on the correlation of the image data with cylinder templates fibre centre lines are generated [15]. Those fibre centre lines are exported as a comma separated value file and the orientation is later mapped on the finite elements. This material orientation mapping allows for one of the simplest segmentation methods, the so called thresholding. Thresholding assigns pixels/voxels based on their grey-scale values to different groups. In this case fibres and matrix can be separated with thresholding. Combining thresholding and fibre tracking creates a fast, automated and very accurate method serving as basis for finite element modelling. This method is called *Thresholding* in this study (Figure 2a). Applying the method *Thresholding* for finite element modelling will deliver accurate stiffness results

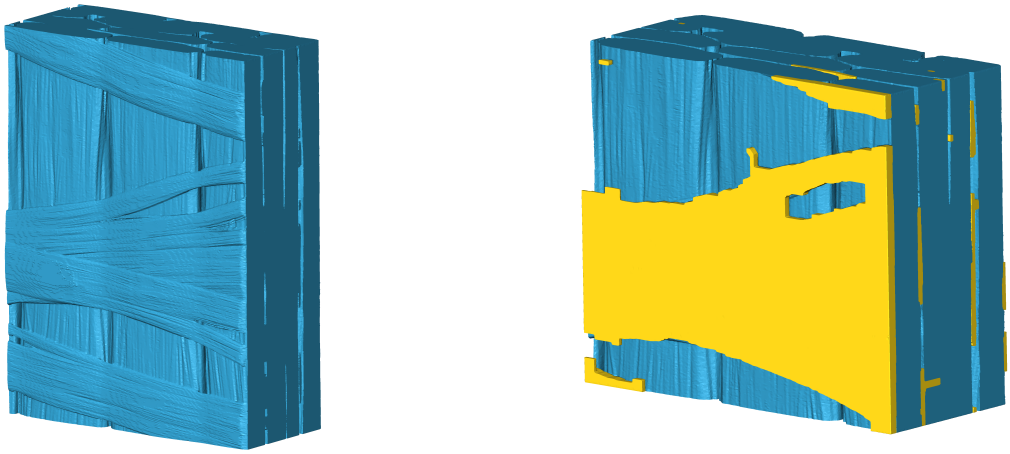

(a) *Thresholding* **(b)** *Physical Boundary*

Figure 2: Automatically segmented surfaces of the methods *Thresholding* and *Physical Boundary* with quasi uni-directional (blue) and backing bundles (yellow) depicted in the commercial software package Avizo™

but can create the drawback that no physical boundary between quasi uni-directional and backing bundles is generated. The resulting stress state at the interface between quasi uni-directional and backing bundles might not be resolved correctly. In order to overcome this issue, advanced morphological operators are applied on the fibre centre lines. With the Avizo™ operators *Dilation*, *Closing* and *Subtract Image* independent backing bundle surfaces are created. This method is called *Physical Boundary* in this study (Figure 2b). Since the operations are not only based on the image data, they can adulterate the actual volume of the uni-directional and backing bundles. The influences of those segmentation choices will be discussed later on in the results of the finite element analysis.

2.4. Modelling

The surface data of both automatically generated segmentations are imported in ANSA™. In this pre-processor mesh quality issues and intersections are removed and a volume mesh of the bundles is created. The meshing of the *Physical Boundary* method takes longer, since penetration issues arise between uni-directional and backing bundles. This segmentation method separates bundles which are very close together. In order to be able to fit in solid elements for the matrix between those bundles a shrinkage of the backing bundles is required. The solid mesh for the matrix surrounding the bundles is generated with the ANSA™ function "Include solid facets in detection". The obtained fibre orientation from AVIZO™ is mapped element-wise onto the solid elements. This ensures accurate stiffness and stress results since the ratio between longitudinal and transverse stiffness with approximately four (Table 1) generates a significant influences of even small misalignments. Figure 3 shows a comparison of the final models.

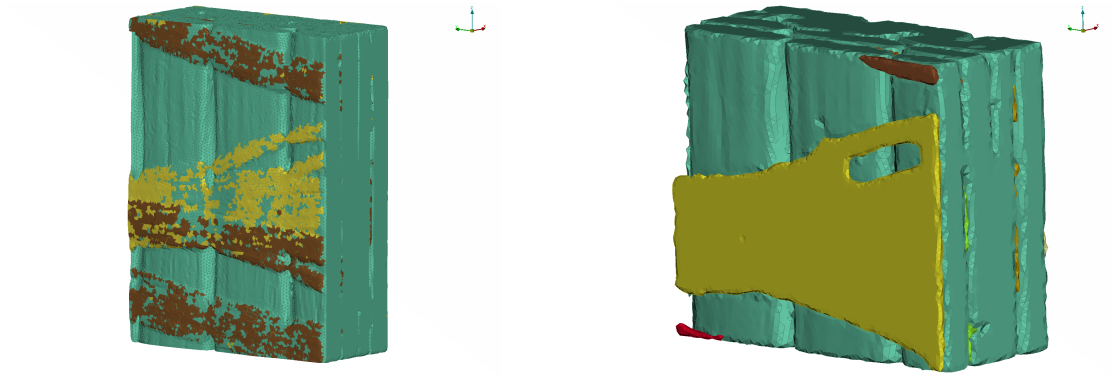

(a) *Thresholding* **(b)** *Physical Boundary*

Figure 3: Meshed models based on the *Thresholding* and *Physical Boundary* segmentation methods with quasi uni-directional (marine-blue) and backing bundles (yellow and brown) depicted in the commercial software package ANSA™. The matrix mesh is masked.

3. Results

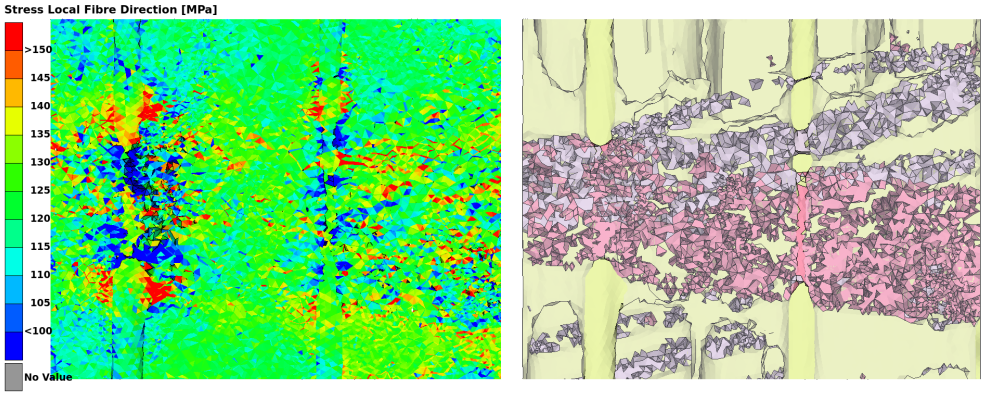

Figure 4: Plane cut of the *Thresholding* model through the volume showing the stresses in fibre direction inside the uni-directional bundles on the left and the position of the overlapping backing bundles on the right.

Both models (*Physical Boundary* and *Thresholding*) were loaded in the main fibre direction with a strain of 0.25 %. Regarding the obtained stress in fibre direction, it becomes clear that there are stress localisations, where backing bundles are crossing uni-directional bundles, depicted in Figure 4. This effect is occurring at all locations where backing bundles and uni-directional bundles are overlaying. Jespersen et al. [16] showed in their study that in this area the fatigue damage process of tension-tension

loaded specimens with a similar material system is originating. They assumed stress concentrations to be the reason for this initial fibre failure. Their theory can be supported by these simulation results. Similar finite element analysis by Jespersen et al. [11] and Blinzler et al. [12] have also shown stress localisations in the overlapping area.

Both models (*Physical Boundary* and *Thresholding*) are able to predict these stress concentrations. There is not significant difference in the stress distribution visible (Figure 5), though areas with higher stresses are more spread in the *Thresholding* model. The

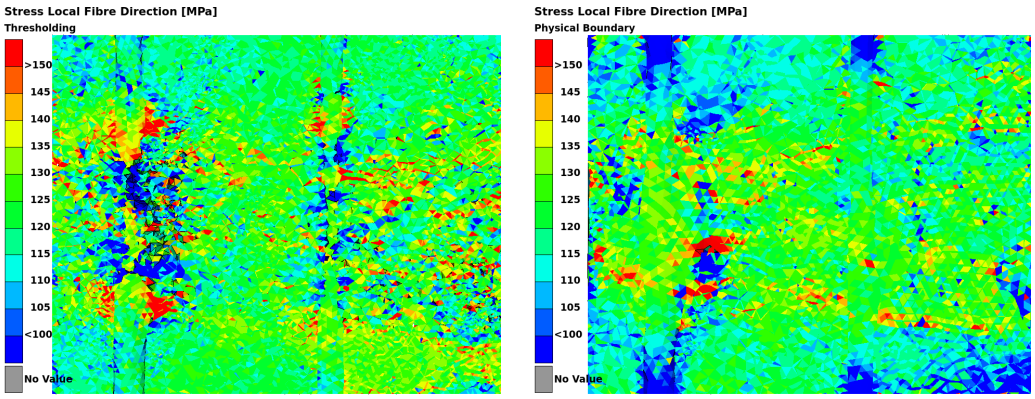

Figure 5: Plane cut through the volume showing the stresses in fibre direction inside the uni-directional bundles. On the left the model based on the segmentation method *Thresholding* is shown, the model on the right bases on the method *Physical Boundary*.

model with the physical boundary representation allows for a smother surface mesh, resulting in a more uniform stress distribution. The model is not able to resolve an effect on the single fibre scale with an average mesh size of 120 μm.

Nevertheless, even on larger scales, stress concentrations are occurring. The stiffness differences between matrix, backing bundles and uni-directional bundles could cause those stress concentrations. By assigning matrix material for the backing bundles in the model based on the segmentation method *Thresholding*, this influence was examined. In other words, the fibres have been virtually removed from the backing bundles. The result is shown in Figure 6. The stress concentrations remain, they are even more severe at this position in the composite. At the other positions of stress concentrations through the volume nearly no differences between the model with backing bundles and the model without backing bundles become visible. By this analysis it becomes evident that the stiffness properties of the backing bundles have no significant influence on the stress localisations inside the uni-directional bundles.

In order to exclude the option, that the observed stress localisations are induced by the mesh, the backing bundles were deleted in the model *Physical Boundary* and the accrued volumes were combined and remeshed as solid matrix elements. The results are depicted in Figure 7. The effect seen in Figure 6 where the concentrated stresses are more spread are visible in this analysis as well. This signifies that, even without the presence of backing bundles in the finite element model, stress concentrations occur.

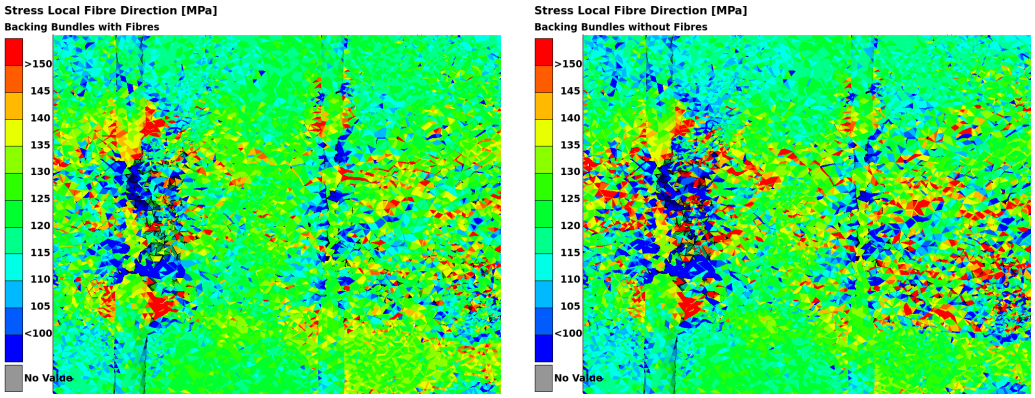

Figure 6: Plane cut through the volume showing the stresses in fibre direction inside the uni-directional bundles. Both models base on the segmentation method *Thresholding*. For the model on the right the material was changed to the matrix material, the model on the left shows the result of the original model with the correct backing bundle stiffness properties (Figure 5 left model).

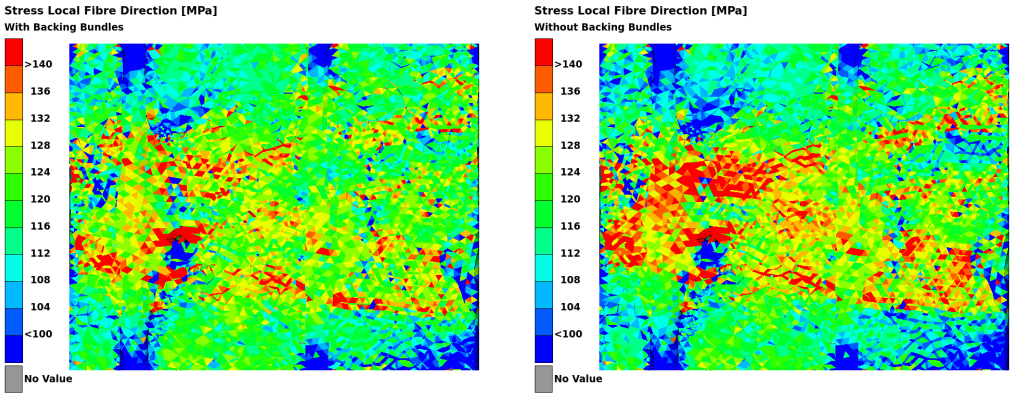

Figure 7: Plane cut through the volume showing the stresses in fibre direction inside the uni-directional bundles. Both models are based on the segmentation method *Physical Boundary*. However, for the model on the right the backing bundles were removed and the accrued volumes were new matrix solid elements. The model on the left shows the result of the original model with the backing bundles included and the correct stiffness properties.

Nevertheless, the waviness of the uni-directional bundles induced due to the backing bundles was not removed. Consequently the waviness is assumed to be the reason for the localised stresses.

It can be concluded that the stress localisations are caused by the backing bundles.

However, not due to different stiffness differences but due to the induced waviness of the uni-directional bundles.

4. Conclusion

In this study the influence of two automated segmentation approaches for X-ray computer tomographic data on the results of a finite element analysis have been compared. As test specimen, a composite made of non-crimp fabrics comprising four uni-directional bundles stacked on top of each other and held together by smaller off-axis backing bundles, was used. The automated segmentation methodologies were developed in Avizo™ and differ in the generation of a boundary between backing and uni-directional bundles.

It has been shown that both models show stress localisations in the overlapping area of backing and uni-directional bundles which has been observed in experimental studies on a similar material system. Based on further investigations presented in this study, it can be concluded that the stress concentrations originate at least partly from the induced waviness due to the backing bundles. The influence of the single fibre scale was not investigated due to the focus on the fibre bundle level in the finite element model.

Since no significant influences of the segmentation method on the finite element analysis has been detected, it can be concluded that the developed automated segmentations are robust. The method *Thresholding* is regarded favourable due to a higher time efficiency and reduced complexity. In future work, the proposed methodology needs to be tested on other composite layups as well. Further research applying the process of transferring X-ray computer tomography images to finite element models is necessary to investigate the origin of the stress concentration on the single fibre scale.

Acknowledgements

This study was funded by EU Horizon 2020 Marie Skłodowska-Curie Actions Innovative Training Network: MUltiscale, Multimodal and Multidimensional imaging for EngineeRING (MUMMERING), Grant Number 765604 and the Erna and Victor Hasselblad foundation grant for female scientists. Financial support from VINNOVA (the Swedish Innovation Agency) via LIGHTer Academy is also gratefully acknowledged. The computations were performed on resources provided by Chalmers Centre for Computational Science and Engineering (C3SE). The X-Ray computer tomography data was acquired using the Zeiss Xradia 520 Versa from the DTU (Technical University of Denmark) Centre for Advanced Structural and Material Testing (CAS-MAT), grant no. VKR023193 from Villum Fonden. At DTU in Roskilde the scanning electron microscopy images were taken. The support of Dr. Eng. Ioannis Nerantzis form BETA CAE Systems SA, Greece and Dr. Jan Giesebrecht from Thermo Fisher Scientific GmbH, Germany is acknowledged.

References

[1] Mikkelsen L P 2020 The fatigue damage evolution in the load-carrying composite laminates of wind turbine blades. *In Fatigue Life Prediction of Composites and Composite Structures* 2nd ed (Elsevier Ltd., Duxford, United Kingdom) 569–603 URL `http://dx.doi.org/10.1016/B978-0-08-102575-8.00016-4`

[2] Mikkelsen L P, Emerson M J, Jespersen K M, Dahl V A, Conradsen K and Dahl A B 2016 X-ray based micromechanical finite element modeling of composite materials *29th Nordic Seminar on Computational Mechanics, Gothenburg, Sweden*
[3] Sharma R, Mahajan P and Mittal R K 2013 Elastic modulus of 3D carbon/carbon composite using image-based finite element simulations and experiments *Composite Structures* **98** 69–78 URL https://10.1016/j.compstruct.2012.11.019
[4] Villarraga-Gómez H, Herazo E L and Smith S T 2019 X-ray computed tomography: from medical imaging to dimensional metrology *Precision Engineering* **60** 544–69 URL https://doi.org/10.1016/j.precisioneng.2019.06.007
[5] du Plessis A, le Roux S G and Guelpa A 2016 Comparison of medical and industrial X-ray computed tomography for non-destructive testing *Case Studies in Nondestructive Testing and Evaluation* **6** 17–25 URL http://dx.doi.org/10.1016/j.csndt.2016.07.001
[6] Maire E and Withers P J 2014 Quantitative X-ray tomography *International Materials Reviews* **59** 1–43 URL https://10.1179/1743280413Y.0000000023
[7] Garcea S, Wang Y and Withers P 2018 X-ray computed tomography of polymer composites *Composites Science and Technology* **156** 305–19 URL https://10.1016/J.COMPSCITECH.2017.10.023
[8] Auenhammer R M, Mikkelsen L P, Asp L E and Blinzler B J 2020 Automated x-ray computer tomography segmentation method for finite element analysis of non-crimp fabric reinforced composites *[Submitted]*
[9] Sencu R M, Yang Z, Wang Y C, Withers P J, Rau C, Parson A and Soutis C 2016 Generation of micro-scale finite element models from synchrotron X-ray CT images for multidirectional carbon fibre reinforced composites *Composites Part A: Applied Science and Manufacturing* **91:1** 85–95 URL https://10.1016/j.compositesa.2016.09.010
[10] Karamov R, Martulli L M, Kerschbaum M, Sergeichev I, Swolfs Y and Lomov S V 2020 Micro-CT based structure tensor analysis of fibre orientation in random fibre composites versus high-fidelity fibre identification methods *Composite Structures* **235** 111818 URL https://10.1016/j.compstruct.2019.111818
[11] Jespersen K M, Asp L E, Hosoi A, Kawada H and Mikkelsen L P 2018 X-ray tomography based finite element modelling of non-crimp fabric based fibre composite *18th European Conference on Composite Materials, Athens, Greece*
[12] Blinzler B J, Wilhelsson D, Asp L E, Jespersen K M and Mikkelsen L P 2018 A Systematic Approach to Transforming Composite 3D Images Into Meso-Scale Computational Models *18th European Conference on Composite Materials, Athens, Greece*
[13] Jespersen K M, Zangenberg J, Lowe T, Withers P J and Mikkelsen L P 2016 Fatigue damage assessment of uni-directional non-crimp fabric reinforced polyester composite using X-ray computed tomography *Composites Science and Technology* **136** 94–103 URL https://10.1016/j.compscitech.2016.10.006
[14] Agarwal B, Broutman L and Chandrashekhara K 2018 *Analysis and performance of fiber composites* 4th ed (Wiley, Hoboken/NJ, USA)
[15] User's guide avizo software 2019 Accessed: 2020-02-25 URL https://assets.thermofisher.com/TFS-Assets/MSD/Product-Guides/users-guide-avizo-software-2019.pdf
[16] Jespersen K M, Glud J A, Zangenberg J, Hosoi A, Kawada H and Mikkelsen L P 2018 Uncovering the fatigue damage initiation and progression in uni-directional non-crimp fabric reinforced polyester composite *Composites Part A: Applied Science and Manufacturing* **109** 481–97 URL https://10.1016/j.compositesa.2018.03.002